

Modeling and Mode Switching Analysis of Electro-hydrostatic Actuators for Primary Flight Control System

GUO Tuanhui^{1,2}, FU Yongling^{1,2}, CHEN Juan^{1,2*}

1. School of Mechanical Engineering and Automation, Beihang University, Beijing 100191, P. R. China;

2. The Laboratory of Aerospace Servo Actuation and Transmission, Beijing 100191, P. R. China

(Received 12 June 2024; revised 16 October 2024; accepted 12 January 2025)

Abstract: With the advancement of more electric aircraft (MEA) technology, the application of electro-hydrostatic actuators (EHAs) in aircraft actuation systems has become increasingly prevalent. This paper focuses on the modeling and mode switching analysis of EHA used in the primary flight control actuation systems of large aircraft, addressing the challenges associated with mode switching. First, we analyze the functional architecture and operational characteristics of multi-mode EHA, and summarize the operating modes and implementation methods. Based on the EHA system architecture, we then develop a theoretical mathematical model and a simulation model. Using the simulation model, we analyze the performance of the EHA during normal operation. Finally, the performance of the EHA during mode switching under various functional switching scenarios is investigated. The results indicate that the EHA meets the performance requirements in terms of accuracy, bandwidth, and load capacity. Additionally, the hydraulic cylinder operates smoothly during the EHA mode switching, and the response time for switching between different modes is less than the specified threshold. These findings validate the system performance of multi-mode EHA, which helps to improve the reliability of EHA and the safety of aircraft flight control systems.

Key words: large aircraft; flight control system; electro-hydrostatic actuator (EHA); mode switching; simulation analysis

CLC number: V227; V245.1

Document code: A

Article ID: 1005-1120(2025)01-0025-12

0 Introduction

The aircraft servo actuation system is a critical component in the flight control system, significantly influencing the aircraft's overall performance, including maneuverability, reliability, and safety^[1-2]. With the development of more electric aircraft (MEA) and all electric aircraft (AEA) technologies^[3-5], traditional hydraulic actuation systems in aircraft onboard actuation systems are gradually being replaced by power-by-wire (PBW) technology^[6-7]. Currently, PBW actuators primarily include electro-hydrostatic actuators (EHAs) and electro-mechanical actuators (EMAs). Due to the risk of jamming, the application of EMA is limited. In contrast, EHA offers high power density, substantial

output, and easy implementation of bypass backups, making it more suitable for use in the primary flight control systems of aircraft^[8-10].

The actuator system of traditional aircraft adopts the form of central hydraulic source and hydraulic servo actuator (HSA), and the hydraulic pipeline is complex and the energy utilization rate is low. The EHA is a typical pump-controlled direct-drive hydraulic system, offering several advantages over traditional valve-controlled systems in terms of efficiency, reliability, and maintainability. When EHA serve as actuators in flight control systems, they are crucial components for achieving flight control, and their performance and reliability are vital for the safety of both the flight control system and

*Corresponding author, E-mail address: chen.juan@buaa.edu.cn.

How to cite this article: GUO Tuanhui, FU Yongling, CHEN Juan. Modeling and mode switching analysis of electro-hydrostatic actuators for primary flight control system [J]. Transactions of Nanjing University of Aeronautics and Astronautics, 2025, 42(1): 25-36.

<http://dx.doi.org/10.16356/j.1005-1120.2025.01.002>

the entire aircraft^[11-12]. To meet reliability requirements, actuators in primary flight control systems are generally arranged with a certain level of redundancy and fault tolerance. As shown in Fig.1, the ailerons and elevators of the A380 aircraft use a parallel redundancy configuration with EHA and HSA^[13-14]. The primary flight control surfaces of the F-35 aircraft employ a dual-redundant EHA^[15].

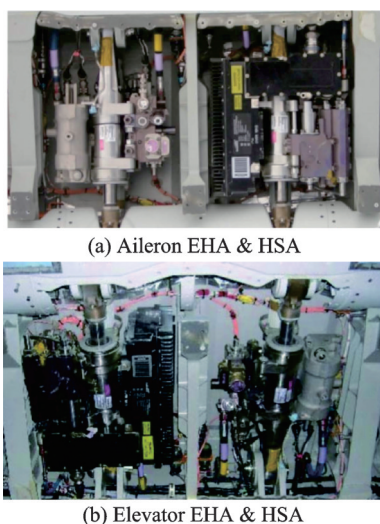


Fig.1 EHA and HSA for the A380 aileron and elevator

As a major development trend for future aircraft actuation systems, enhancing the performance and fault tolerance of EHA has garnered significant attention from scholars both domestically and internationally. Matteo et al.^[16] proposed a comprehensive definition and calculation method for reliability based on the analysis of the structure and characteristics of aircraft actuation systems. They presented a case study on the reliability assessment of SHA/EHA systems. Chen et al.^[17] developed a mathematical model for EHA and identified sensitive parameters for typical failure modes. They further proposed a fault diagnosis method for EHA based on data augmentation techniques, aimed at diagnosing and isolating potential faults. Saeedzadeh et al.^[18] introduced a fault detection and isolation method for EHA based on an updated interactive multiple model approach. The performance of their method was validated through simulations under typical EHA fault conditions. Mo et al.^[19] proposed a fault diagnosis method based on interval analytical redundancy relations and applied this approach to the fault diagnosis

of parametric faults and sensor faults in EHA. Miao et al.^[20] proposed a fault diagnosis method for EHA based on residual generation and deep learning. The performance of this method was validated through comparisons with several classical fault diagnosis methods. Wang et al.^[21] developed a deep convolutional neural network (CNN) for EHA fault diagnosis, comparing its performance against several popular data-driven methods using datasets sampled from the AMESim simulation test platform and experimental test platform. Xin et al.^[22] established a performance degradation model for EHA by analyzing the degradation of various motor parameters. They integrated an adaptive active fault-tolerant control (AFTC) based on radial basis function neural networks, providing a reference for reliability analysis of EHA. Ma et al.^[23] addressed the EHA performance degradation by proposing a prediction method based on time-series generative adversarial networks and CNN-BiLSTM-Attention. This method significantly improved the accuracy of EHA performance predictions.

The aforementioned studies have enhanced the reliability and fault tolerance of EHA from various perspectives. To improve fault tolerance, the parallel EHA used in primary flight control systems typically operates in multiple modes. The parallel actuators driving the primary flight control surfaces of large aircraft generally have more than two operating modes, such as the normal operating mode and the bypass mode. These actuators switch between different modes based on operational requirements. The working mode switching process of EHA need to be fast, accurate and stable, but there is currently limited research on the analysis of mode switching for EHA.

Ge et al.^[24] developed a detailed model of the EHA and conducted a performance analysis, providing theoretical support and simulation validation methods for analyzing the impact of system parameters on control performance. This model places particular emphasis on accounting for the nonlinearities of the servo motor and pump. Yang et al.^[25] developed an EHA model and designed a novel nonlinear variable damping integral sliding mode controller. The effectiveness of the algorithm was verified

through simulation results. Zhao et al.^[26] designed a fault diagnosis and fault-tolerant controller for EHA based on an adaptive neural network robust observer. The control accuracy and robustness of the proposed controller were verified through model simulations. Sang et al.^[27] designed an EHA system to achieve rotational motion of a load, developed a nonlinear simulation model of the EHA, and validated its control performance through both nonlinear simulations and experimental results. The above studies have improved EHA performance by establishing models and conducting simulations to verify the proposed methods. However, these models have not thoroughly addressed the functional modes and mode-switching modeling of the EHA.

This paper aims to model and analyze mode switching in primary flight control EHA based on the principles and system architecture of aviation EHA. Firstly, the functional architecture and operating principles of EHA are summarized. Next, a theoretical mathematical and a simulation model of EHA are developed. Subsequently, the simulation work of EHA is conducted, and the mode switching performance of multi-mode EHA is analyzed. Finally, the conclusions are presented.

In response to the mode switching challenges faced by EHA in large aircraft primary flight control actuation systems, the research contributions and innovation points of this paper are as follows: (1) A comprehensive system model of the EHA was established, with a specific focus on the mode switching functionality. (2) A practical EHA mode-switching process was designed, considering real-world application scenarios. (3) The dynamic performance and system stability during mode switching between different operating modes were analyzed, validating the reliability and robustness of the multi-mode EHA system.

1 Functional Architecture and Working Principle of EHA

EHA system can be categorized into three types based on their control methods: Fixed pump variable motor (FPVM) EHA, fixed motor vari-

able pump (FMVP) EHA, and variable pump variable motor (VPVM) EHA. The FPVM EHA system, composed of a servo motor with adjustable speed, a fixed displacement hydraulic pump, and a hydraulic cylinder. The system flow is adjusted by changing the speed of the servo motor, so as to achieve the purpose of controlling the displacement, speed and output force. The performance of this type of EHA primarily depends on the dynamic performance of the servo motor. With its relatively simple structure and ease of implementation, the FPVM EHA has become a research hotspot and is currently adopted in large aircraft.

This study focuses on FPVM EHA. According to the functional requirements of primary flight control actuation systems, the EHA operate in three modes: Normal operation mode, low damping bypass mode, and high damping bypass mode.

Fig.2 illustrates the principle architecture of the multi-mode EHA system, which consists of controller, driver, servo motor, quantitative pump, pressurized reservoir, mode switching valve group, and hydraulic cylinder, among other components. The anti-cavitation valve and check valve belong to the same type of component, but are named differently based on their functions. The function of the check valves is to draw oil from the high-pressure oil circuit. The pressurized reservoir and anti-cavitation valves form the EHA makeup circuit, ensuring back pressure, preventing cavitation, and compensating for EHA leakage. Safety valves ensure that the working pressure of the EHA does not exceed safe limits. The flow control of this EHA is achieved by servo control, which adjusts the speed and direction of the servo motor and the fixed-displacement piston pump, thereby enabling servo control of the hydraulic cylinder.

The EHA switches between three modes through the mode switching valve group. The mode switching valve group consists of check valves, solenoid valve A, mode valve, adjustable damping valve, bypass valve, and solenoid valve B. The mode valve and the bypass valve are spool valves, while solenoid valve A and solenoid valve B are responsible for controlling the hydraulic control port

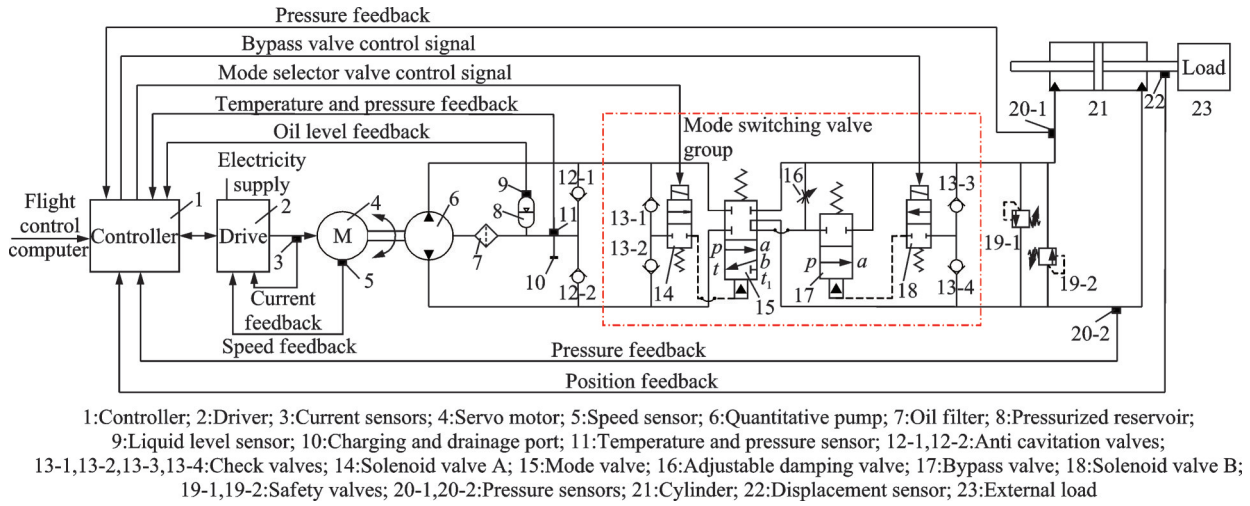


Fig.2 Principle architecture of the multi-mode EHA

pressures of the mode valve and bypass valve, respectively. a, b, p, t, t_1 are hydraulic interfaces.

As shown in Fig.3, the implementation and analysis of the EHA mode switching function are as follows:

(1) Normal operation mode

As shown in Fig.3(a), in this mode, the motor is powered on, the solenoid valve A is energized, and the solenoid valve B is de-energized. Energizing solenoid valve A connects the hydraulic control port of the mode valve to the high-pressure main oil circuit. When the pressure difference between the control oil and the pressurized reservoir exceeds 5 MPa, the mode valve opens, connecting the front and rear main oil circuits. In normal operation mode, the EHA can function as the primary actuator, providing the force necessary to drive the aircraft's control surfaces.

(2) Low damping bypass mode

As shown in Fig.3(b), in this mode, the motor is powered off, the solenoid valve A is de-energized, and the solenoid valve B is energized. The de-energization of solenoid valve A closes the mode valve, while energizing solenoid valve B connects the hydraulic control port of the bypass valve to the high-pressure chamber of the hydraulic cylinder. When the pressure difference between the control oil and the pressurized reservoir exceeds 5 MPa, the bypass valve opens, directly connecting the two chambers of the hydraulic cylinder. In the low damping bypass mode, the two chambers of the hydraulic

cylinder are directly connected, and the EHA can function as a backup actuator, with the piston rod following the movement of the aircraft's control surfaces. This mode is also known as the follow-up mode or backup mode.

(3) High damping bypass mode

As shown in Fig.3(c), in this mode, both the motor and solenoid valves are powered off. The solenoid valve A is de-energized, closing the mode valve, and the solenoid valve B is de-energized, closing the bypass valve. In this configuration, the

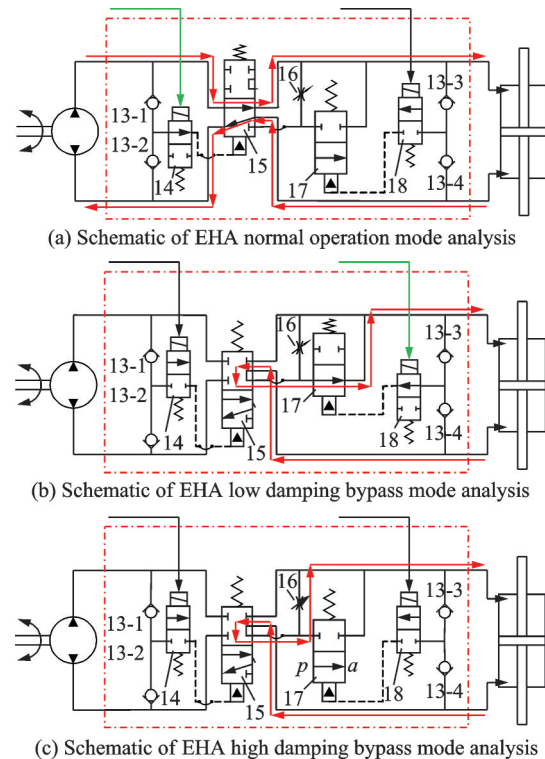


Fig.3 Schematic of EHA mode switching analysis

two chambers of the hydraulic cylinder are connected via an adjustable damping valve. When a failure occurs and the EHA cannot operate normally, it switches to a high damping bypass mode, and the piston rod moves slowly, following the movement of the aircraft's control surfaces. The unpowered EHA typically operates in this mode.

2 Modeling of EHA

2.1 Mathematical model

2.1.1 Mathematical model of the servo motor

The EHA adopts a permanent magnet synchronous motor (PMSM) as its driving component, typically utilizing a surface-mounted PMSM. To achieve high-performance control of the motor, the Park and Clark transformations are employed to convert the current and voltage from the three-phase coordinate system to the d -axis and q -axis coordinate system of the motor. The voltage equations of the PMSM in the rotating d - q coordinate system are given by

$$\begin{cases} U_d = R i_d + L_d \frac{di_d}{dt} - \omega_e L_q i_q \\ U_q = R i_q + L_q \frac{di_q}{dt} + \omega_e (L_d i_d + \psi_f) \end{cases} \quad (1)$$

where U_d and U_q represent the stator voltages along the d and q axes, respectively; i_d and i_q the stator currents along the d and q axes, respectively; and L_d and L_q the stator inductances along the d and q axes, respectively. R is the stator resistance; ω_e the electrical angular velocity of the motor; and ψ_f the magnetic flux of the permanent magnet.

The electromagnetic torque equation for the PMSM is expressed as

$$T_e = \frac{3}{2} p [\psi_f + (L_d - L_q) i_d] i_q \quad (2)$$

where T_e is the electromagnetic torque of the PMSM, and p the number of pole pairs of the PMSM.

2.1.2 Mathematical model of the hydraulic pump

To enhance the thermal management of the EHA, the wet motor technology has emerged as a prominent research focus. By integrating the rotor of

the PMSM with the main shaft of the piston pump into a single coaxial design, an integrated motor-pump unit is formed. This unit serves as the hydraulic power source for the EHA. The motion equation of the integrated motor-pump can be expressed as

$$J_m \frac{d\omega_m}{dt} = T_e - B_m \omega_m - D_p (p_a - p_b) \quad (3)$$

where J_m is the rotational inertia of the motor-pump rotor, B_m the viscous friction coefficient of the motor-pump, ω_m the mechanical angular velocity of the motor pump, and D_p the displacement of the piston pump. p_a and p_b are the pressures at the hydraulic pump's outlet and inlet ports, respectively.

Considering the internal and external leakage of the EHA hydraulic pump, as well as the compressibility of the hydraulic fluid, the flow rate equation can be expressed as

$$\begin{cases} Q_a = D_p \omega_m - Q_{ip}(p_a, p_b) - Q_{olpa}(p_a, p_{ac}) - \frac{V_a}{\beta_e} \frac{dp_a}{dt} \\ Q_b = D_p \omega_m - Q_{ip}(p_a, p_b) + Q_{olpb}(p_b, p_{ac}) + \frac{V_b}{\beta_e} \frac{dp_b}{dt} \end{cases} \quad (4)$$

where Q_a and Q_b are the flow rates at the outlet and inlet ports of the motor-pump, respectively. Q_{ip} is the internal leakage flow rate of the pump; Q_{olpa} the external leakage flow rate at the pump outlet; Q_{olpb} the external leakage flow rate at the pump inlet; p_{ac} the replenishment pressure from the pressurized reservoir; and β_e the bulk modulus of the hydraulic fluid. V_a and V_b are the equivalent volumes of the outlet and inlet chambers, respectively.

2.1.3 Mathematical model of the hydraulic cylinder

The hydraulic oil entering the cylinder is primarily used to drive piston movement. Additionally, it must compensate for internal leakage and the compressibility of the hydraulic fluid. Considering the internal leakage of the hydraulic cylinder while neglecting external leakage, the dynamic flow rate equation for the hydraulic cylinder is expressed as

$$\begin{cases} Q_1 = A \frac{dx}{dt} + \frac{V_{10} + Ax}{\beta_e} \frac{dp_1}{dt} + Q_{ilc}(p_1, p_r) \\ Q_r = A \frac{dx}{dt} - \frac{V_{r0} - Ax}{\beta_e} \frac{dp_1}{dt} + Q_{ilc}(p_1, p_r) \end{cases} \quad (5)$$

where Q_1 and Q_r denote the inflow and outflow rates

of the two chambers of the hydraulic cylinder, respectively; p_l and p_r the pressures in the left and right chambers of the hydraulic cylinder; and V_{l0} and V_{r0} the volumes of the sealed chambers on the two sides of the hydraulic cylinder, respectively. Q_{ic} stands for the internal leakage flow rate of the hydraulic cylinder, A the effective piston area in the hydraulic cylinder, and x the displacement of the piston rod.

The piston rod of the hydraulic cylinder moves in response to hydraulic pressure, overcoming both viscous frictional forces and external loads. The motion equation for the hydraulic cylinder can be expressed as

$$M_c \frac{d^2 x}{dt^2} = A(p_l - p_r) - B_c \frac{dx}{dt} - K_s x - F_f - F_{ex} \quad (6)$$

where M_c represents the equivalent mass acting on the piston rod, B_c the viscous friction coefficient of the hydraulic cylinder, K_s the elastic load coefficient,

F_f the static frictional force, and F_{ex} the external load.

In the normal operation mode of an EHA, the pressure loss caused by the flow passages within the valve block is neglected due to their short length. Based on the principle of continuity of flow, it follows that

$$\begin{cases} Q_l = Q_a \\ Q_r = Q_b \\ p_l = p_a \\ p_r = p_b \end{cases} \quad (7)$$

In the bypass mode of an EHA, the hydraulic cylinder chambers are interconnected adhering to

$$\begin{cases} Q_l = Q_r \\ p_l = p_r \end{cases} \quad (8)$$

2.2 AMESim simulation model

Based on the mathematical model analysis, the simulation model of the EHA was constructed using AMESim software, as depicted in Fig.4. Two c_1

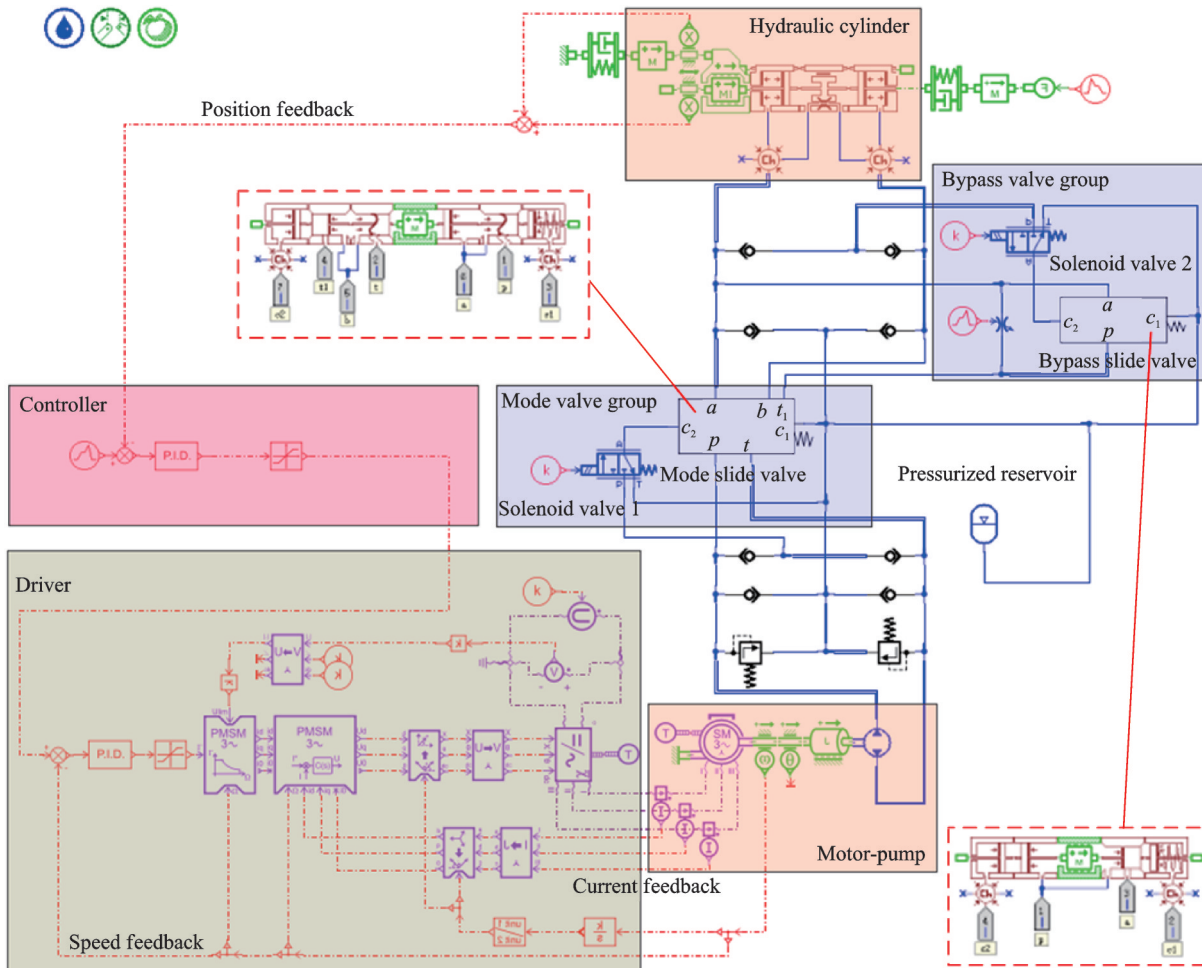


Fig.4 Simulation model of EHA

represent the valve core oil discharge ports corresponding to the hydraulic control ports c_2 of the mode valve and bypass valve, and c_1 is directly connected to the booster oil tank.

Considering the nonlinearity of the model and the accuracy of the modeling, models for the mode valve, bypass valve, and hydraulic cylinder were established using the HCD library. Both the mode valve and bypass valve are spool valves, encapsulated as subcomponents.

3 Simulation Experiment

3.1 Simulation of normal operation mode

Setting the EHA system to its normal operation mode, wherein the solenoid valve A is powered, the p port and a port of the mode valve are interconnected, while the b port and t port are interconnected. According to the application requirements of the EHA, simulate its performance under three operating conditions: No load, power point, and maximum force, as well as sinusoidal response characteristics.

The primary simulation parameters of the EHA are listed in Table 1.

Table 1 Primary simulation parameters

| Parameter | Value |
|--|------------------|
| Stator resistance/ Ω | 0.093 |
| d -axis inductance/ mH | 0.456 |
| q -axis inductance/ mH | 0.456 |
| Rotor inertia/ ($\text{kg}\cdot\text{m}^2$) | $2.26\text{e}-4$ |
| Viscous friction coefficient/ ($\text{Nm}\cdot(\text{r}\cdot\text{min}^{-1})^{-1}$) | $1.67\text{e}-4$ |
| Pump displacement/ ($\text{mL}\cdot\text{r}^{-1}$) | 1.845 |
| Maximum speed/ ($\text{r}\cdot\text{min}^{-1}$) | 13 000 |
| Cylinder diameter/ mm | 72.85 |
| Piston rod diameter/ mm | 34.87 |
| Cylinder stroke/ mm | ± 51 |
| Fixed-end dead zone volume/ cm^3 | 29.4 |
| Moving-end dead zone volume/ cm^3 | 12.5 |
| Viscous friction coefficient/ ($\text{N}\cdot(\text{m}\cdot\text{s}^{-1})^{-1}$) | 10 000 |

For the no-load condition, provide a step position command with an amplitude of 50 mm to the EHA. For the power point condition, apply a load

force of 30 000 N to the EHA and provide a step position command with an amplitude of 50 mm. For the maximum force condition, apply a load force of 100 000 N to the EHA after it stabilizes in position. The position command and load force are shown in Fig.5.

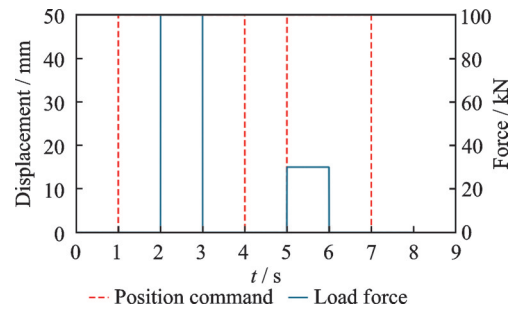


Fig.5 Position command and load force of EHA

During the sinusoidal response test of the EHA, provide a position command of ± 2.5 mm and a frequency of 6.5 Hz under no-load conditions, and observe the position output response of the EHA.

3.2 Simulation and analysis of EHA model switching performance

The mode switching process of the EHA is determined based on the potential switching scenarios encountered in practice. An EHA that is not powered typically remains in the high damping bypass mode.

When the EHA is powered on for normal operation mode, it switches from the high damping bypass mode to the normal operation mode. If the EHA switches from the operational mode to the backup mode, it switches from the normal operation mode to the low damping bypass mode. Conversely, when switching from the backup mode to the operational mode, it switches from the low damping bypass mode to the normal operation mode. In the event of a failure during normal operation, the EHA switches from the normal operation mode to the high damping bypass mode.

During this process, the EHA operates under the power point condition in its normal operation mode. In both the high damping bypass mode and the low damping bypass mode, a load force of 20 000 N is applied to the piston rod.

4 Results and Discussion

As shown in Fig.6, during the no-load step response, the rise time of the EHA position is approximately 0.343 s, with overshoot less than 0.5 mm and steady-state position error within ± 0.05 mm, meeting the system performance requirements. The maximum linear velocity of the hydraulic cylinder under no-load conditions can reach 115 mm/s, fulfilling the requirements for aircraft primary flight control surfaces.

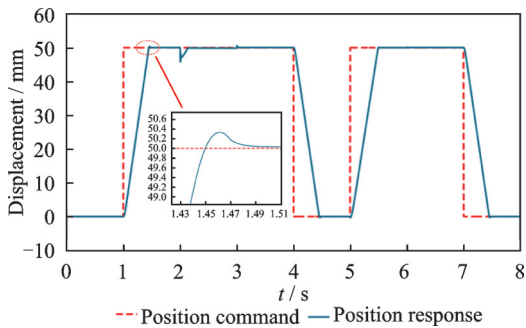


Fig.6 Position command and response of EHA

From Fig.6, it can be observed that after applying a load force of 100 000 N at the 2nd second, the EHA exhibits negative displacement due to the impact of the load. However, the position response returns to steady state after approximately 0.15 s, with a steady-state position error within ± 0.05 mm. When the load force is removed at the 3rd second, there is a slight fluctuation in the position response of the EHA. Overall, the analysis indicates that the EHA can maintain system stability under maximum output force conditions.

As depicted in the latter part of Fig.6, at the 5th second, the EHA responds to a step input of 50 mm under a load force of 30 000 N. The rise time, overshoot, and steady-state position error of the EHA meet the system performance requirements. The maximum linear velocity of the hydraulic cylinder under load conditions is 108 mm/s, indicating excellent actuation capability of the EHA under load.

The sinusoidal response of the EHA, as shown in Fig.7, indicates that the phase lag of the EHA position response is 2.88° , with the amplitude attenuating to 2.43 mm, which is 97% of the command val-

ue. The tracking of the command is satisfactory, and the EHA bandwidth exceeds 6 Hz.

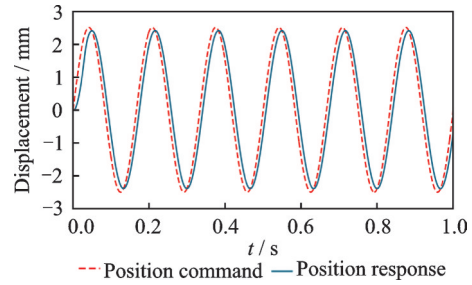


Fig.7 Sine response of EHA position

In summary, the performance indicators of the EHA under the three conditions of no load, maximum force, and power point meet the system requirements, with a bandwidth exceeding 6 Hz. The analysis results demonstrate the excellent performance of the EHA under normal operation conditions, indicating the accuracy and practicality of the model constructed. Additionally, it lays the foundation for the subsequent analysis of the EHA's state switching performance.

The operation of the mode valve and bypass valve for different mode switching is achieved by controlling solenoid valves. The control commands of the solenoid valve A and the solenoid valve B, along with the spool displacement responses of the mode valve and bypass valve, are depicted in Fig.8.

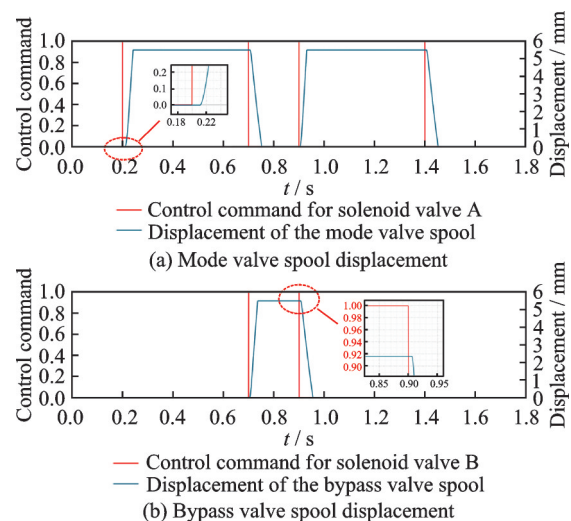


Fig.8 Response curves of mode valve and bypass valve spool displacement

Simulation results demonstrate that when switching from high damping bypass mode to normal operation mode, the mode valve opens with a

response time of 42 ms. Conversely, switching from normal operation mode to low damping bypass mode sees the mode valve closing in 53 ms, while the bypass valve opens in 36 ms. When shifting from low damping mode to normal operation mode, the bypass valve closes in 55 ms, and the mode valve opens in 32 ms. Switching from normal operation mode to high damping bypass mode results in the mode valve closing in 53 ms. All switching time mentioned are below 60 ms, indicating that the mode-switching performance of the EHA meets the required criteria.

From the results in Fig.8, it can be observed that the switching of the mode valve and bypass valve requires a certain process. Notably, the spool displacement response of the mode valve and bypass valve exhibits a significant delay relative to the control commands of the solenoid valve. A more detailed analysis of the mode valve switching process is provided. As shown in Fig.9, during the process of the mode valve being actuated by the solenoid valve A, the pressure response at the hydraulic control port of the mode valve lags behind the control command of the solenoid valve. As the pressure at the hydraulic control port increases sufficiently to overcome the preload of the mode valve spring, the spool of the mode valve begins to move. Therefore, the initiation of the mode valve spool movement is delayed by approximately 10 ms relative to the solenoid valve control command. The mode valve spool takes approximately 32 ms to complete its movement, after which the pressure at the hydraulic control port of the mode valve rapidly increases and stabilizes, holding the mode valve in the fully open po-

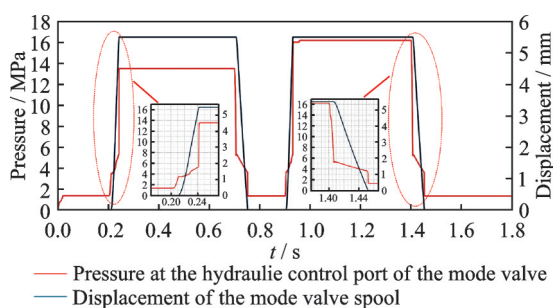


Fig.9 Hydraulic control port pressure curve and spool displacement curve of the mode valve

sition. The total response time for the mode valve to open is 42 ms.

As shown in Fig.9, during the process of solenoid valve A controlling the closure of the mode valve, the pressure at the hydraulic control port of the mode valve drops rapidly, with a swift response. The spool of the mode valve only begins to move when the pressure at the hydraulic control port falls below the spring force of the mode valve. Consequently, the initiation of spool movement is delayed by approximately 6 ms relative to the control command of the solenoid valve. The spool of the mode valve takes approximately 47 ms to reach its final position, after which the pressure at the hydraulic control port quickly decreases to its minimum. Under the action of the spring preload, the spool stabilizes in the closed position. The total response time for the mode valve to close is 53 ms. From this, it can be concluded that the mode valve opens faster than it closes. The opening and closing processes of the bypass valve follow the same pattern as those of the mode valve.

Analyzing the system characteristics during the switching process of the EHA, the piston rod displacement curve in Fig.10 indicates that the hydraulic cylinder operates smoothly before and after mode switching. A comparison of the displacement responses during the four mode switching processes shows that fluctuations in hydraulic cylinder pressure significantly affect the stability of the EHA during the mode switching process.

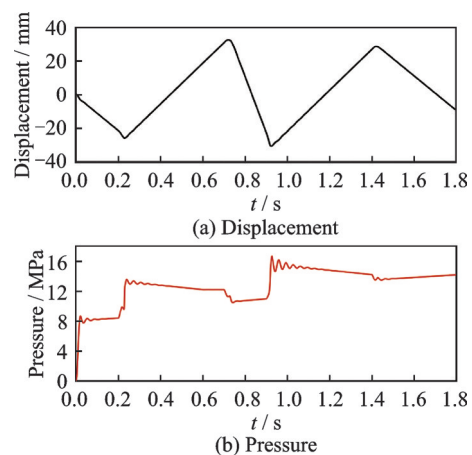


Fig.10 Piston rod displacement curve and left chamber pressure curve of the EHA

The performance of mode switching is a crucial prerequisite for the successful application of EHA in aircraft primary flight control systems. The research validates the mode switching performance of EHA based on possible real-world scenarios. This study enhances the reliability and safety of EHA application in aircraft flight control systems from the perspectives of mode switching and redundancy backup.

5 Conclusions

This study investigates the mode switching of EHA in aircraft primary flight control systems, and the following conclusions are drawn:

(1) A theoretical mathematical model and an AMESim simulation model of the EHA with multiple operating modes have been established. The models focus on the implementation methods and performance characteristics of mode switching in EHA.

(2) Through the analysis of the EHA performance under three typical operating conditions, it is demonstrated that the EHA exhibits high control accuracy and excellent load-bearing capabilities. Additionally, the EHA's sinusoidal command tracking performance is satisfactory, with a system bandwidth exceeding 6 Hz.

(3) The mode switching function of the EHA can be adapted to actual application scenarios, allowing for seamless switching between different operating modes. During the switching process, the response time of the EHA is consistently below 60 ms, meeting the requirements for system performance. The outstanding mode switching performance of EHA contributes to enhancing the reliability and safety of aircraft flight control systems.

References

- [1] ALLE N, HIREMATH S S, MAKARAM S, et al. Review on electro hydrostatic actuator for flight control[J]. *International Journal of Fluid Power*, 2016, 17(2): 125-145.
- [2] FENG Y, SUN Z H, WU L N, et al. Nonlinear adaptive flight control system: Performance enhancement and validation[J]. *Chinese Journal of Aeronautics*, 2023, 36(4): 354-365.
- [3] BUTICCHI G, WHEELER P, BOROYEVICH D. The more-electric aircraft and beyond[J]. *Proceedings of the IEEE*, 2023, 111(4): 356-370.
- [4] JIANG Jun, LI Zhi, LI Wenyuan, et al. A review on insulation challenges towards electrification of aircraft[J]. *High Voltage*, 2023, 8(2): 209-230.
- [5] MARE J C, FU J. Review on signal-by-wire and power-by-wire actuation for more electric aircraft[J]. *Chinese Journal of Aeronautics*, 2017, 30(3): 857-870.
- [6] MARE J C. Review and analysis of the reasons delaying the entry into service of power-by-wire actuators for high-power safety-critical applications[J]. *Actuators*, 2021, 10(9): 233.
- [7] JIAO Zongxia, YU Bo, WU Shuai, et al. An intelligent design method for actuation system architecture optimization for more electrical aircraft[J]. *Aerospace Science and Technology*, 2019, 93: 105079.
- [8] HAO Zhenyang, ZHANG Qiyao, CHEN Huajie, et al. Research and design of coordinated control strategy for smart electromechanical actuator system[J]. *Transactions of Nanjing University of Aeronautics and Astronautics*, 2022, 39(5): 507-520.
- [9] GUO T H, HAN X, MINAV T, et al. A preliminary design method of high-power electro-hydrostatic actuators considering design robustness[J]. *Actuators*, 2022, 11(11): 308.
- [10] FU Y L, HAN X, SEPEHRI N, et al. Design and performance analysis of position-based impedance control for an electrohydrostatic actuation system[J]. *Chinese Journal of Aeronautics*, 2018, 31(3): 584-596.
- [11] JIAO Zongxia, LI Zhihui, Shang Yaoxing, et al. Active load sensitive electro-hydrostatic actuator on more electric aircraft: Concept, design, and control[J]. *IEEE Transactions on Industrial Electronics*, 2022, 69(5): 5030-5040.
- [12] DERMOUCHE R, TALAOUBRID A, BARAZANE L, et al. Qualitative and quantitative analysis of the reliability of NPC and ANPC power converters for aero-nautical applications[J]. *Alexandria Engineering Journal*, 2022, 61(6): 4863-4873.
- [13] BOSSCHED V. The A380 flight control electro-hydrostatic actuators achievements and lessons learnt[C]// *Proceedings of the 25th Congress of the International Council of the Aeronautical Sciences*. Hamburg, Germany: ICAS, 2006.
- [14] MARE J C. *Aerospace actuators 3: European commercial aircraft and tiltrotor aircraft*[M]. Great Britain and the United States: ISTE Ltd and John Wiley & Sons Inc, 2018.

- [15] ROBBINS D, BOBALIK J, STENA D D, et al. F-35 subsystems design, development, and verification [M]. [S.l.]: American Institute of Aeronautics and Astronautics, 2019: 365-398.
- [16] MATTEO D L, BERRI P C, BONANNO G, et al. Fault detection and identification method based on genetic algorithms to monitor degradation of electrohydraulic Servomechanisms[C]//Proceedings of the 4th International Conference on System Reliability and Safety. Rome, Italy: Institute of Electrical and Electronics Engineers, 2019: 304-311.
- [17] CHEN Huanguo, MIAO Xu, MAO Wentao, et al. Fault diagnosis of EHA with few-shot data augmentation technique[J]. *Smart Materials and Structures*, 2023, 32(4): 4005.
- [18] SAEEDZADEH A, HABIBI S, ALAVI M, et al. A robust model-based strategy for real-time fault detection and diagnosis in an electro-hydraulic actuator using updated interactive multiple model smooth variable structure filter[J]. *Journal of Dynamic Systems, Measurement, and Control*, 2023, 145(10): 101006.
- [19] MO Haobin, LI Yanjun. Fault diagnosis based on interval analytic redundancy relation[J]. *Journal of Nanjing University of Aeronautics & Astronautics*, 2021, 53(6): 972-980.(in Chinese)
- [20] MIAO Jianguo, WANG Jianyu, WANG Dong, et al. Experimental investigation on electro-hydraulic actuator fault diagnosis with multi-channel residuals[J]. *Measurement*, 2021, 180: 109544.
- [21] WANG Jianyu, MIAO Jianguo, WANG Jinglin, et al. Fault diagnosis of electrohydraulic actuator based on multiple source signals: An experimental investigation[J]. *Neurocomputing*, 2020, 417: 224-238.
- [22] XIN Zhaozhou, WANG Shaoping, ZHANG Chao. Establishment of EHA performance degradation model based on PMSM and its active fault tolerant control[C]//Proceedings of the 31st European Safety and Reliability Conference. Angers, France: Singapore, 2021: 3117-3124.
- [23] MA Zhonghai, SUN Yiwen, JI Hui, et al. A CNN-BiLSTM-Attention approach for EHA degradation prediction based on time-series generative adversarial network[J]. *Mechanical Systems and Signal Processing*, 2024, 215: 111443.
- [24] GE Yaowen, ZHU Weilin, LIU Jiahui, et al. Refined modeling and characteristic analysis of electro-hydrostatic actuator[J]. *Journal of Mechanical Engineering*, 2021, 57(24): 66-73.
- [25] YANG Rongrong, ZHANG Ling, ZHAO Jiali, et al. Nonlinear variable damping integral sliding mode control for electro-hydrostatic actuator[J]. *Journal of Beijing University of Aeronautics and Astronautics*, 2024, 50(1): 163-172.(in Chinese)
- [26] ZHAO Jieyan, HU Jian, YAO Jianyong, et al. EHA fault diagnosis and fault tolerant control based on adaptive neural network robust observer[J]. *Journal of Beijing University of Aeronautics and Astronautics*, 2023, 49(5): 1209-1221.(in Chinese)
- [27] SANG W J, JI W B, JU H K. EHA modeling and control with hydraulic cylinder parallel motion[C]//Proceedings of the 26th International Conference on Mechatronics Technology. Busan, Korea: Institute of Electrical and Electronics Engineers, 2023.

Acknowledgement The work was supported by the Chinese Civil Aircraft Project (No.MJ-2017-S49).

Authors

The first author Mr. GUO Tuanhui is a Ph.D. candidate in School of Mechanical Engineering and Automation of Beihang University. He focuses on modeling and digital twins of mechatronic systems, as well as intelligent health management of equipment.

The corresponding author Dr. CHEN Juan received the Ph.D degrees in School of Automation Science and Electrical Engineering from Beihang University, Beijing, China. She is currently an associate professor at School of Mechanical Engineering and Automation from Beihang University. Her research interest contains reliability and risk management of complex systems, storage life extension and accelerated life testing and servo system health management.

Author contributions Mr. GUO Tuanhui designed the study, compiled the models, conducted the analysis, interpreted the results and wrote the manuscript. Prof. FU Yongling contributed to the background and design of the study and provided project support. Dr. CHEN Juan contributed to the analysis of the results and provided constructive suggestions for the revision of the study. All authors commented on the manuscript draft and approved the submission.

Competing interests The authors declare no competing interests.

(Production Editor: SUN Jing)

主飞控电静液作动器的建模和模式切换分析

郭团辉^{1,2}, 付永领^{1,2}, 陈娟^{1,2}

(1. 北京航空航天大学机械工程及自动化学院, 北京 100191, 中国;

2. 航天伺服驱动与传动技术实验室, 北京 100191, 中国)

摘要:随着飞机多电化(More electric aircraft, MEA)技术的发展,电静液作动器(Electro-hydrostatic actuators, EHAs)在飞机作动系统中的应用越来越广泛。针对EHA在大型飞机主飞控作动系统中应用涉及的模式切换问题,开展飞机主飞行控制EHA的建模和模式切换分析研究。首先,对多工作模式EHA的功能架构和工作特点开展分析,总结EHA的工作模式和实现方式。之后,基于EHA的体系架构,建立EHA的理论数学模型和仿真模型。接下来,基于仿真模型对EHA正常运行时的性能进行分析。最后,结合功能切换场景研究了EHA在模式切换过程中的性能表现。结果表明,EHA在精度、带宽和带载能力方面满足性能要求,且EHA在模式切换过程中液压缸运行平稳,在不同工作模式之间切换的响应时间均小于指标要求。研究结果验证了多模式EHA的系统性能,有助于提升EHA的可靠性及飞机飞行控制系统的安全性。

关键词:大型飞机;飞行控制系统;电静液作动器;模式切换;仿真分析